ORIGINAL ARTICLE

Veterinary Research Forum. 2026; 17 (3): 207 - 216
doi: 10.30466/vrf.2025.2048535.4585
Journal Homepage: vrf.iranjournals.ir

Veterinary Research Forum

Genetic diversity of H9N2 avian influenza viruses in Iran over the past two decades

Mohsen Bashashati*, Soroush Geramitabar, Setareh Banani, Leila Moradihaghgou, Fereshteh Sabouri

Department of Avian Disease Research and Diagnostics, Razi Vaccine and Serum Research Institute, Agricultural Research Education and Extension Organization (AREEO), Karaj, Iran.

Article Info

Article history:

Received: 22 January 2025
Accepted: 22 April 2025
Available online: 15 March 2026

Keywords:

Avian influenza virus
Complete genome sequencing
Evolutionary analysis
Iran

Abstract

Numerous studies have explored the molecular epidemiology of H9N2 viruses in Iran; however, continuous monitoring remains vital for timely interventions to mitigate potential damage. This study examined the molecular characteristics and evolutionary features of Iranian H9N2 viruses by sequencing the complete genomes of two viruses, Marand and Baneh, isolated in 1998 and 2022, respectively, alongside other Iranian strains from GenBank. All Iranian viruses were identified as low-pathogenic avian influenza viruses, as evidenced by the presence of the di-basic motif K/RSSR cleavage site. Notably, all Iranian viruses isolated from 2009 onward had an L at position 216 in the hemagglutinin receptor binding site, whereas earlier viruses exhibited a Q/L at the same position, an essential mutation that enhances replication in mammalian cells. The molecular evolutionary rates for the Iranian *hemagglutinin* (*HA*) and *neuraminidase* (*NA*) genes were estimated at 4.50×10^{-3} and 3.60×10^{-3} substitutions *per* site *per* year, respectively. Error-prone replication of H9N2 viruses has resulted in the continuous evolution of Iranian strains over two decades, characterized by three phases of population growth. Maximum likelihood phylogenetic analysis revealed that the *HA* and *NA* genes of H9N2 viruses from domestic chickens belonged to the G1 sublineage. Additionally, the internal genes of some viruses displayed evidence of reassortment with other subtypes, indicating potential gene exchange with other viruses. These findings underscored the importance of ongoing surveillance of H9N2 viruses in both domestic and wild bird populations, given the human-like receptor-binding preference and the possibility of genetic reassortment with various viral subtypes.

Introduction

Avian influenza (AI) is a highly contagious respiratory disease caused by the *Alphainfluenzavirus influenzae* of the *Orthomyxoviridae* family.[1] The *Anseriformes* and *Charadriiformes* orders serve as key biological and genetic reservoirs for AI viruses (AIVs). The AIVs are classified into 18 hemagglutinin (HA) and 11 neuraminidase (NA) subtypes.[2] With the exception of two influenza-like viruses found in bats (H17N10 and H18N11), all subtypes have been identified in both domestic and wild birds.[3] The AIVs are further categorized based on their pathogenicity in poultry: high pathogenicity AI (HPAI) viruses cause severe, systemic illness and high mortality in bird flocks, whereas low pathogenicity AI (LPAI) viruses generally cause subclinical or mild infections, primarily affecting the respiratory and reproductive systems.[2]

Since its first identification in turkeys in 1966, the H9N2 virus has been found predominantly in shorebirds and wild ducks. The 1990s saw widespread outbreaks of H9N2 across various regions, affecting a range of avian species.[4] Since 1998, H9N2 outbreaks have been reported in the Middle East, significantly affecting commercial chicken populations. Although classified as LPAI, H9N2 can lead to substantial economic losses through reduced egg production and increased mortality, especially when coupled with other infections. The virus can also cross species barriers, infecting mammals such as humans and pigs. The first human case of H9N2 was reported in Hong Kong in 1999 and sporadic cases have since occurred.[5,6]

The H9N2 viruses are divided into two main lineages: North American and Eurasian. The Eurasian lineage was further divided into the G1-, Y280-, Y439-, and F/98-sublineages. Studies have shown that among the H9N2

***Correspondence:**

Mohsen Bashashati. DVM, DVSc
Department of Avian Disease Research and Diagnostics, Razi Vaccine and Serum Research Institute, Agricultural Research Education and Extension Organization (AREEO), Karaj, Iran.
E-mail: m.bashashati@rvsri.ac.ir

viruses circulating between 1998 and 2009, four groups (A, B, C, and D) were identified. Phylogenetic analysis using maximum likelihood methods of the *HA* and *NA* genes revealed that genotypes B and D, originating from the G1-like sublineage, were prevalent in Iran from 2003 to 2009 and from 1998 to 2007, respectively.[7] Multiple H9N2 introductions occurred in Iran between 1998 and 2019, resulting in four well-supported monophyletic groups. Viruses from subgroups 2 - 4 clustered in genetic group B of the G1 sublineage with isolates from Afghanistan, Iraq, and Pakistan, whereas early isolates from 1998 - 2007 fell into Group D.[8]

The presence of H9N2 viruses alongside other HPAI strains in wild bird populations in Iran, combined with immunological pressure from vaccination, increases the risk of new reassortant viruses emerging.[9] Despite the availability of inactivated H9N2 vaccines since the first official report of the virus in Iran, outbreaks continue to occur, even in vaccinated flocks. Given these concerns, molecular and phylogenetic analyses of circulating H9N2 strains are crucial. This study aimed to analyze the genetic diversity of Iranian H9N2 viruses, identify their molecular properties and characterize their evolutionary patterns over more than two decades, with a particular focus on two representative H9N2 strains from this period.

Materials and Methods

Viruses. Two H9N2 viruses, namely Marand and Baneh, were obtained from the Department of Avian Disease Research and Diagnostics at the Razi Vaccine and Serum Research Institute. The Marand virus was initially isolated from industrial chicken farms in Tehran province and was used as the first inactivated vaccine seed at Razi Vaccine and Serum Research Institute, Iran largest vaccine manufacturer, until 2021 when it was replaced by a newer strain. During passive surveillance in 2022, the Baneh virus was detected in samples (trachea and lung) collected from 26-day-old broilers in Baneh which suffered severe respiratory symptoms and high mortality rates. The vaccination history of this farm is unknown and other common pathogens (Newcastle disease and infectious bronchitis viruses) were not detected in the samples. Both H9N2 viruses were propagated and harvested from the allantoic sacs of nine-day-old specific pathogen-free embryonated chicken eggs (Venkys, Pune, India). After confirming the presence of H9N2 in the allantoic fluids by RT-PCR, the samples were stored at – 70.00 ˚C for further use.

RNA extraction and reverse transcription polymerase chain reaction (RT-PCR). Viral genomic RNA was extracted from allantoic fluid using the High Pure Viral RNA Kit (Roche Diagnostics, Mannheim, Germany). Reverse transcription was then performed using the Uni12 primer (AGC AAA AGC AGG) and a biotechrabbit™ cDNA Synthesis Kit (Biotechrabbit GmbH, Berlin, Germany) following the manufacturer's instructions. The full-length genomes of H9N2 viruses were amplified as previously described methods.[10] The PCR products were excised from the gels and purified using the GeneJET Gel Extraction Kit (Thermo Fisher Scientific, Waltham, USA).

Genomic sequencing. Each purified PCR product was ligated into the pJET1.2/blunt cloning vector (CloneJET PCR Cloning Kit, Thermo Fisher Scientific) according to the instructions, and the ligation mixture was transformed into *Escherichia coli* TOP10 competent cells by incubating them at 42.00 ˚C for 1 min. The transformed cells were then plated on Luria-Bertani agar containing 100 µg mL^{-1} ampicillin. Colony PCR was used to screen bacterial transformants for the presence of target genes. Positive clones were cultured overnight in Luria-Bertani broth with 100 µL mL^{-1} ampicillin, and DNA was extracted using the High Pure Plasmid Isolation Kit (Roche Diagnostics). Sanger sequencing was performed using an Applied Biosystems® 3500 genetic analyzer (Thermo Fisher Scientific) and the BigDye™ Terminator v3.1 cycle sequencing kit (Thermo Fisher Scientific) according to the manufacturer's instructions. Internal primers were designed to sequence the polymerase and *HA* genes (primer sequences available upon request).

Sequence and phylogenetic analysis. The raw sequences were compiled and edited using the BioEdit (version 7.2; Ibis Therapeutics, Carlsbad, USA).[11] The most closely related sequences were retrieved from the EpiFlu database (Global Initiative on Sharing All Influenza Data) and the NCBI influenza virus sequence database. The sequences most closely related to the eight segments of the studied H9N2 viruses were identified using a BLAST search. The MAFFT (version 7.0; online server https://mafft.cbrc.jp/alignment/server/) was used to align consensus sequences, which were then trimmed to an equal length for each gene. Phylogenetic analysis was conducted using the maximum likelihood method with 1,000 bootstrap replicates, based on the complete coding sequences of each gene segment, in MEGA (version 12.0; Biodesign Institute, Tempe, USA).[12] Potential N-linked glycosylation sites (NGSs) in the *HA* and *NA* genes were predicted using the NetNGlyc 4.0 server (https://services.healthtech.dtu.dk/services/NetOGlyc-4.0/). The three-dimensional structure of the HA protein was modeled using the HA protein structure of H9N2 (PDB ID: 1JSD) in SWISS-MODEL (https://swissmodel.expasy.org/) and visualized using PyMOL Molecular Graphics System, version 3.1.3 (Schrödinger, New York, USA).

Recombination analysis. To account for the potential impact of recombinant sequences on phylogenetic and selection pressure analyses, the sequences were evaluated using the RDP (version 4.101).[13] Recombination was considered valid when detected using at least three different methods and such sequences were excluded from the final dataset.

Selection pressure analysis. To assess selection pressure on the codons of the surface glycoprotein genes (*HA* and *NA*), the ratio of non-synonymous to synonymous mutations (ω) was calculated using four methods: Mixed Effects Model of Evolution (MEME), Fast Unconstrained Bayesian Approximation (FUBAR), Fixed Effects Likelihood (FEL), and Single-Likelihood Ancestor Counting (SLAC) on the data monkey platform (http://www.data-monkey. org/). A ratio of ω < 1 indicated negative selection, ω = 1 suggested neutral evolution, and ω > 1 implied positive selection. Sites under positive selection were identified if they were supported by at least three of the four methods: p < 0.1 for the MEME, FEL, and SLAC, or posterior probability > 0.9 for the FUBAR.

Evolutionary dynamic analysis. To estimate the time to the most recent common ancestor (tMRCA), evolutionary rate, and evolutionary dynamics of Iranian H9N2 AIVs, the HA and NA sequences were subjected to Bayesian Markov chain Monte Carlo (MCMC) analysis using the BEAST v1.10.4.[14] All sequences were tip-dated based on the year of virus isolation using BEAUti v1.10.4.[14] Given the superior performance of the SRD06 nucleotide substitution model, the datasets were analyzed under an uncorrelated lognormal relaxed clock model using the General Time Reversible substitution model with gamma-distributed rate variation among sites (GTR+G). The MCMC chain was run for 100 million steps, with samples taken every 1,000 generations. Convergence and adequate mixing of the chains were assessed using Tracer version 1.7.2, ensuring that all estimated parameters had effective sample size (ESS) values greater than 200.[15] Maximum clade credibility (MCC) trees were generated from the tree posterior distribution using TreeAnnotator v1.10.4, discarding the first 10.00% of samples as burn-in.[14] The MCC trees were visualized using FigTree v1.4.4 (https:// tree.bio.ed.ac.uk/software/figtree/), which enabled estimation of tMRCA for each gene. The demographic history of Iranian H9N2 viruses was examined using Gaussian Markov Random Field (GMRF) Bayesian skyride plot model. The results were visualized by the Tracer.[15]

Nucleotide sequence accession numbers. The nucleotide sequences of all eight gene segments of the Baneh and Marand H9N2 viruses were submitted to GenBank under accession numbers PV390722 to PV390737.

Results

Homology analysis. The *M* and *NS* genes exhibited high nucleotide sequence similarity (92.00 - 93.50%), whereas the *NP* gene exhibited high amino acid sequence identity (98.10%). Genetic comparisons of the *HA* and *NA* genes revealed that the two viruses shared 89.00% nucleotide identity and 87.60 - 90.80% amino acid identity. In comparison with the Marand virus, the polymerase segments of the Baneh strain demonstrated 89.20 - 90.60% nucleotide sequence identity and 95.20 - 97.40% amino acid similarity. According to the BLAST search results, the Marand H9N2 virus clustered closely with Iranian H9N2 viruses isolated in 1998. The ribonucleoprotein complex genes (*PB2*, *PB1*, *PA*, and *NP*) of Baneh virus were most homologous to H7N9 and H9N2 subtypes from China. The nucleotide sequences of the other genes in this virus were more closely related to H9N2 isolates from Middle Eastern countries including Iraq and Pakistan.

Molecular characterization. The deduced amino acid sequences of the viral proteins were analyzed to identify molecular determinants related to host adaptation, virulence and drug resistance. Analysis of the HA protein revealed two distinct protease cleavage site motifs in the studied H9N2 isolates. The Baneh strain exhibited the consensus sequence ^{317}KSSR^{320} (H9 numbering throughout the manuscript) while the Marand strain displayed the motif ^{317}RSSR^{320}, both characteristic of LPAI viruses. Furthermore, at position 216, the Baneh virus had leucine, whereas the Marand virus had glutamine. This substitution at position 216 in the HA receptor-binding site is known to enhance virus binding to α2,6-linked sialic acid, increasing replication efficiency in mammalian cells and ferrets.[16,17] This mutation has been consistently observed in Iranian H9N2 viruses since 2009 (data not shown) and appears to have become permanent due to positive selection pressure. Additionally, several amino acids associated with antigenic epitopes on the HA protein of H9 AIVs were identified.[18-22] Compared to the Marand strain, the Baneh virus exhibited nine amino acid substitutions within HA antigenic sites, which may alter viral antigenicity (Fig. 1).

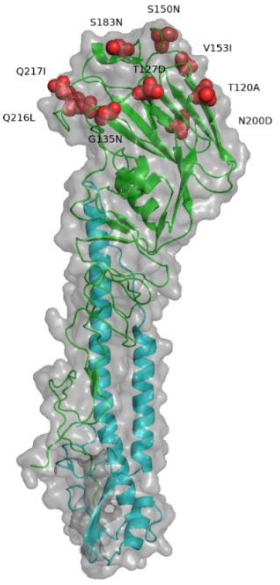

Fig. 1. Mutations in the HA antigenic sites of the Baneh virus compared to the Marand virus. The location of H9 mutations is shown as red spheres with H9 numbering.

While no mutations conferring resistance to NA inhibitors were detected, confirming the viruses' susceptibility to these drugs, the Marand strain displayed an L26F mutation in the M2 protein, indicating potential resistance to adamantane derivatives. In contrast, all known mutations associated with adamantane resistance (L26F, V27A, A30T, A30V, S31N, and G34E) were absent in the more recent Baneh virus.[23] The predicted NGSs of the HA proteins of Marand and Baneh viruses were identical, with six potential NGSs (N-X-S/T) at positions 11, 87, 123, 280, 287, and 474. However, although both viruses contained six NGSs in the NA protein, the patterns differed. The Marand virus had NGSs at positions 61, 69, 70, 86, 146, and 234, but the glycosylation sites at positions 70 and 86 were absent in the recent virus. Notably, the Baneh virus had an additional potential glycosylation site at position 44.

Positive selection of the Iranian HA and NA proteins. The selection profiles of the Iranian HA and NA proteins are shown in Table 1. Analysis of the ratio of synonymous to non-synonymous substitution rates indicated the presence of purifying (negative) selection ($\omega < 1$) for both proteins, with only a few positively selected sites detected (Table 1). Amino acid positions 180, 216, and 264 of the HA protein were consistently identified by FEL, FUBAR, MEME, and SLAC as positively selected sites. Similarly, residue 317 of the NA protein was identified as positively selected.

Evolutionary analysis. The molecular evolutionary rates of the Iranian *HA* and *NA* genes were estimated to be 4.50×10^{-3} and 3.60×10^{-3} substitutions *per* site *per* year, respectively, indicating that the *HA* gene mutates more rapidly. The tMRCA estimates for the *HA* and *NA* genes of the Iran-1, Iran-2, and Iran-4 groups were similar, but for the Iran-3 group, different tMRCA values were observed for the *HA* and *NA* genes (Table 2). This might be due to the availability of more HA than NA sequences during certain periods. Two GMRF skyride plots were generated to assess the demographic history of Iranian H9N2 viruses over two decades, revealing three phases of growth (Fig. 2). The results showed an increase in viral diversity from 1998 to 2003 following the introduction of the H9N2 virus into Iran, followed by a reduction from 2004 to 2010, likely due to vaccination efforts. Diversity increased again in 2011, followed by a slight decrease over the next five years. Both genes exhibited a third phase of increasing diversity starting around 2016. However, viral diversity has remained constant since late 2017.

Phylogenetic analysis of surface genes. The Phylogenetic relationships among H9N2 strains were analyzed based on the eight viral gene segments (Figs. 3 and 4). The HA and NA maximum likelihood phylogenetic trees were constructed using sequenced genes and selected sequences from Iran and other regions, representing all sublineages (Fig. 3). The phylogenetic topology of both surface genes indicated that they grouped within the G1 sublineage and shared a common ancestor with A/quail/Hong Kong/G1/1997 strain. The Baneh virus, along with the current H9N2 vaccine strain, was clustered into the Iran-4 group (2011 - 2019).[8] Phylogenetic analyses of the *MP* gene revealed that all Iranian H9N2 viruses (except for those from wild birds) were

Table 1. Nucleotide positions in the hemagglutinin (HA) and neuraminidase (NA) proteins of Iranian H9N2 viruses that are under positive selection. Numbers in bold are positive selection sites by four mentioned approaches.

Models*	HA protein†				NA protein			
	FEL	FUBAR	MEME	SLAC	FEL	FUBAR	MEME	SLAC
Global dN/dS	0.217				0.253			
No. of codon sites	548				469			
No. of positive selection sites	4	3	24	3	6	2	16	1
Positively selected sites	150, **180**, **216**, **264**	**180**, **216**, **264**	2, 3, 6, 9, 73, 90, 102, 139, 150, **180**, 202, 203, 207, **216**, 217, 246, 248, 249, **264**, 299, 370, 486, 517, 520	**180**, **216**, **264**	16, 30, 37, 249, **317**, 328	**317**, 328	16, 30, 37, 42, 70, 99, 107, 216, 227, 228, 249, 316, **317**, 318, 319, 424	**317**

dN/dS: Ratio of non-synonymous to synonymous mutations; FEL: Fixed effects likelihood; FUBAR: Fast unconstrained Bayesian approximation; MEME: Mixed effects model of evolution; SLAC: Single- likelihood ancestor counting.

* FEL, MEME and SLAC with *p*-value threshold of 0.10, and FUBAR, with posterior probability over 0.90 were considered statistically significant.

† Residues are in H9 numbering except underlined sites in which numbering begin from methionine of H9.

Table 2. Estimated evolution rates and most recent common ancestor (tMRCA) of *Hemagglutinin (HA)* and *neuraminidase (NA)* genes of Iranian H9N2 viruses

Surface glycoprotein genes	HA	NA	HA	NA
	Mean		95.00% highest posterior density	
Iranian groups	4.50×10^{-3}	3.60×10^{-3}	4.00×10^{-3} - 5.10×10^{-3}	3.00×10^{-3} - 4.20×10^{-3}
	Mean tMRCA		95.00% highest posterior density interval	
Iran-1	Jun 1995	Jun 1995	Oct 1993 - Oct 1996	Sep 1993 - Nov 1996
Iran-2	Aug 2001	Aug 2002	Jul 2000 - Jun 2002	Aug 2000 - Apr 2004
Iran-3	Nov 2006	Nov 2003	May 2005 - Feb 2008	Mar 2001 - Nov 2005
Iran-4	Apr 2009	Oct 2009	May 2007 - Feb 2011	Feb 2006 - Jul 2012

closely related and grouped within the G1 sublineage. In the *NP* gene phylogenetic tree, the studied H9N2 viruses were clustered into two distinct sublineages: F/98 and Y439. Phylogenetic analysis of the *PB1* and *PA* genes of Baneh virus provided evidence of reassortment with other viral subtypes (H7N9), suggesting that H9N2 viruses might have donated internal genes to generate reassortant viruses capable of infecting humans.[24]

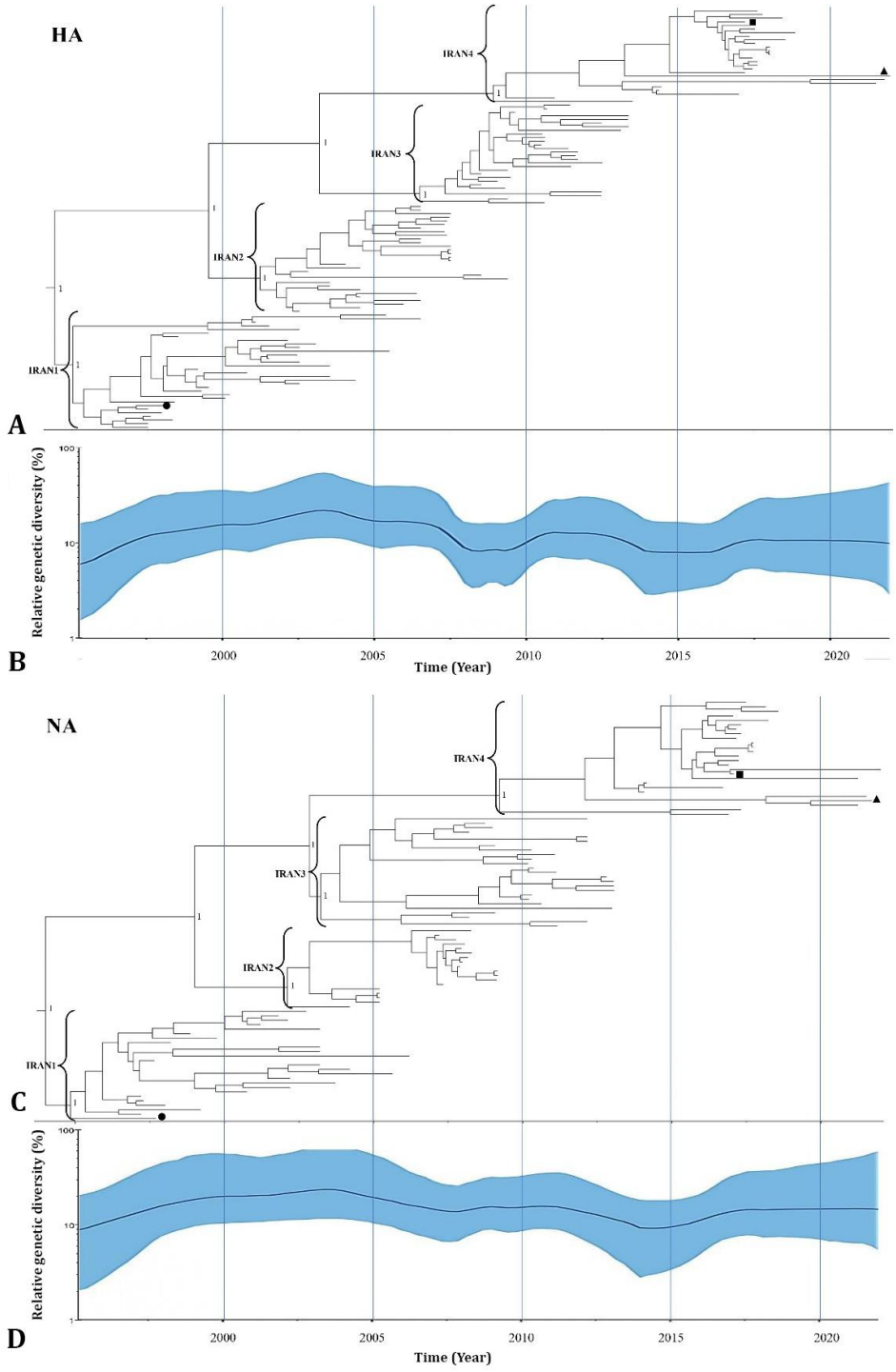

Fig. 2. Time-resolved phylogenetic trees constructed using the Bayesian MCMC method and GMRF Bayesian skyride plots showing changes in EPS of the *HA* and *NA* genes of Iranian H9N2 viruses. **A)** HA phylogenetic tree; **B)** HA skyride plot; **C)** NA phylogenetic tree; and **D)** NA skyride plot. In the phylogenetic trees (A, C), the scale bar indicates time in years. The Marand virus is marked with a black circle, the Baneh virus with a black triangle, and the current vaccine strain with a black square. In the skyride plots (B, D), the solid black line represents the median EPS, and the blue shaded area indicates the 95.00% highest posterior density (HPD) interval.

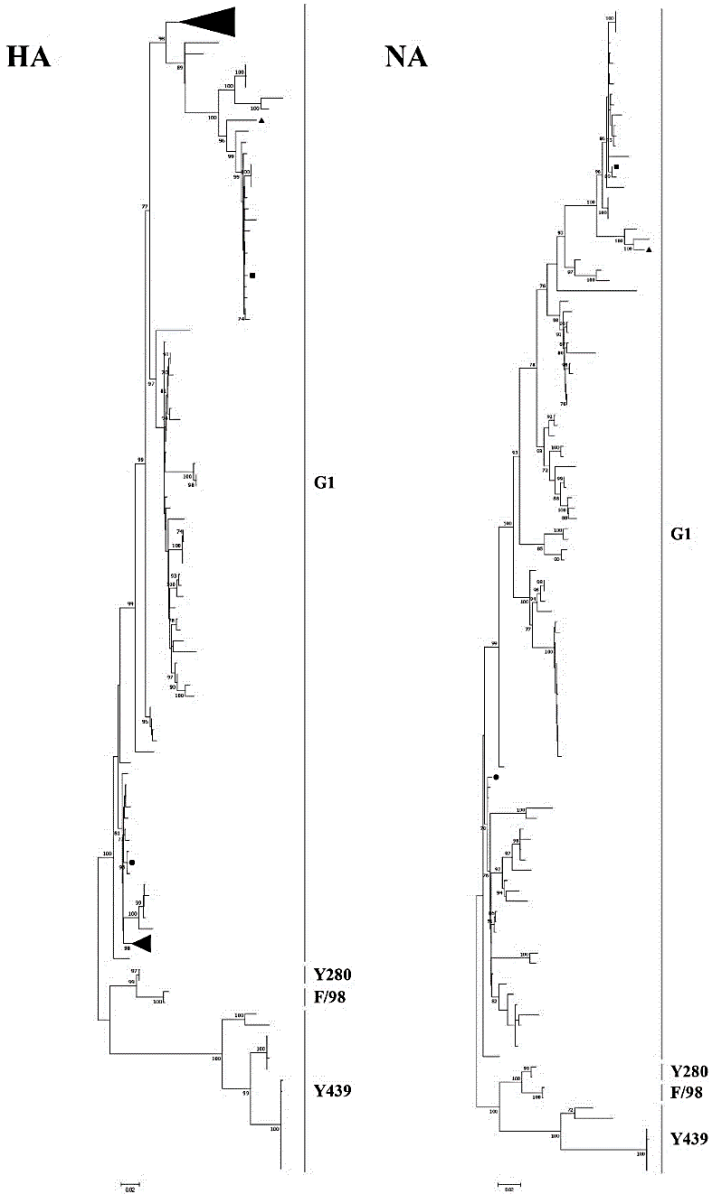

Fig. 3. Maximum likelihood phylogenetic trees of the surface glycoproteins (HA and NA) of H9N2 viruses. The Marand virus is marked with a black circle, while the Baneh virus is marked with a black triangle. The current vaccine strain is indicated by a black square. Vertical lines denote the H9N2 sublineages. The phylogenetic tree was constructed using all available Iranian H9N2 virus sequences from GenBank. The Y280 and F/98 sublineages have not been identified in Iran.

Discussion

H9N2 vaccination strategies have been widely implemented to reduce the impact of this disease on poultry production. Despite the extensive use of inactivated vaccines, H9N2 AIV remains endemic causing repeated outbreaks and significant economic losses in the poultry industry. This ongoing challenge is partly due to the virus's high mutation rate driven by the error-prone activity of its viral polymerase, which underscores the need for continuous genetic and antigenic monitoring of vaccine strains to maintain their effectiveness against circulating viral variants.[25]

In 2021, Razi Vaccine and Serum Research Institute, responsible for supplying 350 million doses (covering 40.00% of the country's needs), replaced its primary vaccine strain, the Marand virus, with a newer strain. This update, the first in two decades, was selected for its close genetic and antigenic match to the circulating H9N2 viruses in Iran. Nonetheless, ongoing surveillance is essential to evaluate the genetic and antigenic characteristics of emerging virus strains. This study aimed to analyze the genetic diversity of Iranian H9N2 viruses, with a particular focus on the Marand and Baneh strains, to identify molecular features and evolutionary dynamics of these viruses over the past two decades.

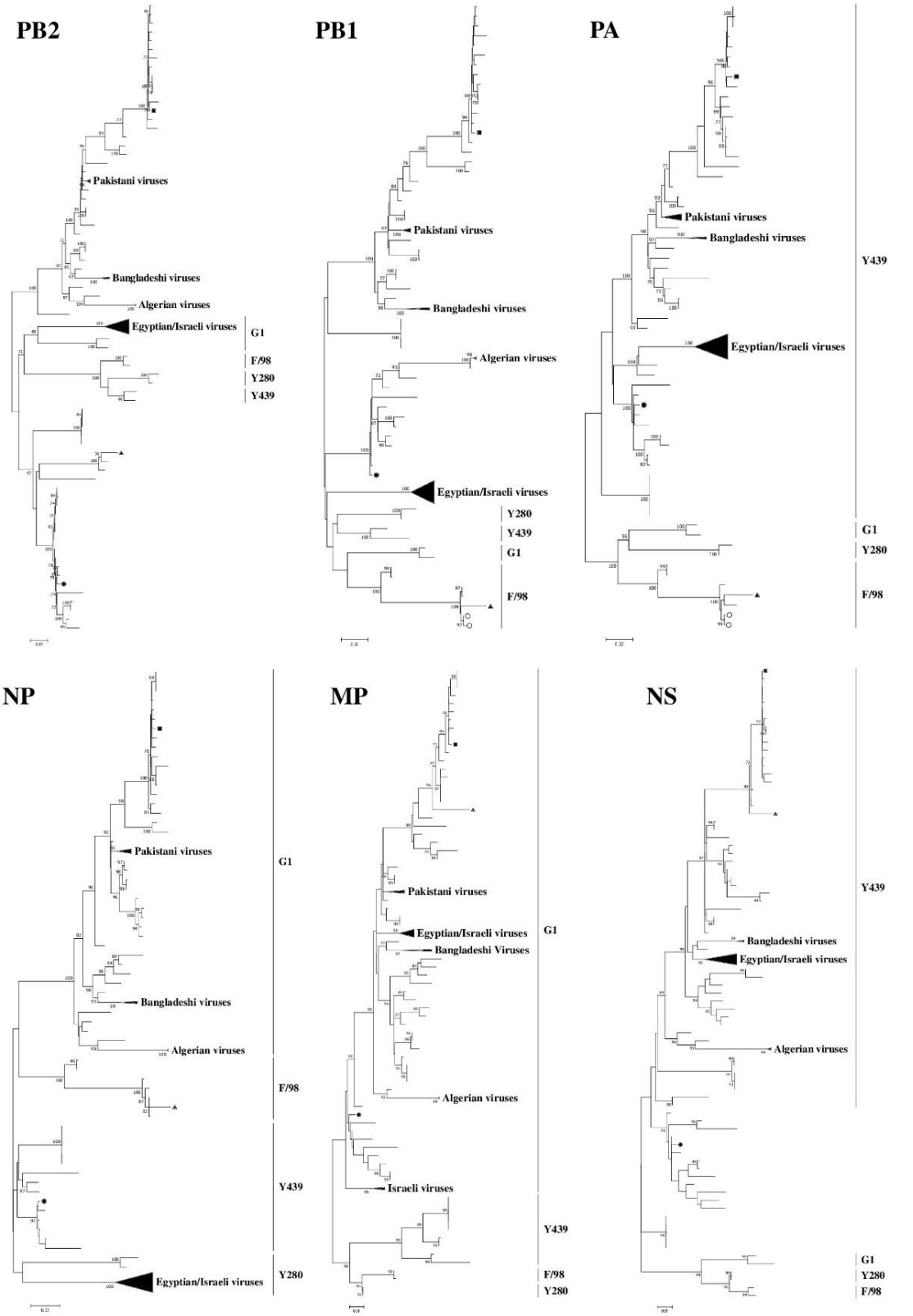

Fig. 4. Maximum likelihood phylogenetic trees of the internal genes (*PB2*, *PB1*, *PA*, *NP*, *MP*, and *NS*) of H9N2 viruses. The Marand virus is marked with a black circle, while the Baneh virus is marked with a black triangle. The current vaccine strain is indicated by a black square. H7N9 viruses are represented by empty circles. Vertical lines denote the H9N2 sublineages. Bootstrap values greater than 70.00% are shown to support the nodes.

The H9N2 viruses can act as donors of partial or full gene cassettes to produce novel, human-infecting re-assortants such as H5N1, H7N9, H10N8, H5N6, H6N1, H7N4, and H3N8 viruses.[26] Conversely, H9N2 viruses may also acquire single or multiple genes from HPAI strains, such as H5N1 and H7N3.[24] A close relationship was observed between the Baneh ribonucleoprotein complex and other AI subtypes identified in China. In Iran, a similar genetic identity has been found between the *M* and *NS* genes of H9N2 and Pakistani H7N3 viruses.[9] Although the H7Nx subtype has not yet been detected in Iran, it might have been introduced through bird migration as Iran lies within a major migratory flyway and participates in international poultry trade. Similarly, the glycoprotein genes of the Baneh strain exhibited a high degree of similarity to H9N2 isolates from Pakistan and Iraq, high-lighting the significance of these neighboring countries in the genetic exchange and spread of H9N2 viruses.

The amino acid sequence at the cleavage site of all Iranian viruses, including the Marand and Baneh strains, lacks multiple basic amino acids, indicating LPAI. Notably, the Baneh virus shows a preference for binding to human receptors due to the Q216L mutation, distinguishing it from the Marand virus.[27] This mutation has been reported in several studies in Iran. Previous research identified leucine at position 216 in the receptor-binding site of the HA protein in H9N2 viruses isolated in Iran.[8,9,28,29] No mutations associated with resistance to NA inhibitors were observed in the studied H9N2 viruses, indicating susceptibility to these drugs. However, while Baneh virus did not exhibit mutations linked to amantadine resistance, Marand virus exhibited the L26F mutation. A single-point mutation at positions 26, 27, 30, 31, or 34 of the M2 protein can confer resistance to adamantanes.[23]

The NGSs in the HA and NA proteins can either positively or negatively affect the pathogenicity of the AIV, depending on their location.[30] Both Marand and Baneh viruses exhibited six NGSs with identical HA protein patterns. However, differences in NGS profiles were observed between the NA proteins of the two viruses. The impact of the two missing glycosylation sites in Baneh and the presence of an additional glycosylation site at a different position relative to the Marand virus requires further investigation.

In our analysis of Iranian HA proteins, three positively selected sites (positions 180, 216, and 264) were consistently identified across the four algorithms with most other sites showing neutral or purifying selection pressures. Among these, antigenic residue 180, which influences significant antigenic variation among natural H9N2 viruses, affects HI titers by altering antibody-epitope recognition rather than changing receptor-binding avidity. Moreover, at position 216, the substitution between Q and L impacts HI titers by altering receptor-binding avidity because it is located within the receptor-binding site. Shi *et al.* studied the *HA* genes of H9N2 subtypes from various hosts and found that, although most sites were subject to neutral or purifying selection, a small number of sites in antigenic regions and receptor-binding sites showed positive selection.[31] The limited number of sites under positive selection for H9N2 viruses may result from several factors. Previous studies on influenza viruses have suggested that positive selection was often linked to antigenic variation and adaptation to new hosts.[32] The identification and use of these positively selected sites (180, 216, and 264) provides insights into antigenic drift and offers critical information for vaccine design and effectiveness against evolving H9N2 strains.

Various studies have investigated the molecular evolutionary rates of the *HA* and *NA* genes of H9N2 viruses in Iran.[8,28] Bashashati *et al.* reported a progressive increase in genetic variability in the *HA* genes, whereas, the *NA* genes showed relatively consistent levels of variability, as evidenced by Bayesian skyline plots, which contradicts the results of this study.[28] The GMRF skyride plots of the *HA* and *NA* genes of Iranian H9N2 viruses generated in this study suggested that the initial phase likely reflected the virus's establishment and adaptation within a newly introduced avian population. The decline in genetic diversity observed between 2004 and 2010 may indicate that vaccination efforts successfully reduced the prevalence of specific H9N2 variants, resulting in a more genetically uniform viral population. However, the increase in the number of cases observed in 2011 may be due to factors such as antigenic drift, which allows certain viral variants to evade immunity conferred by earlier vaccines. The stabilization observed since late 2017 may suggest a new equilibrium between ongoing viral mutations and selective pressures that may be potentially influenced by continued vaccination programs or changes in poultry husbandry practices.

The evolutionary analysis of H9N2 viruses isolated in Iran, with a focus on strains from 1998 and 2022, underscored the dynamic nature of these viruses and their potential implications for poultry health. Phylogenetic analysis revealed that current Iranian H9N2 strains belong predominantly to the G1-like sublineage, emphasizing the importance of continuous surveillance and potential updates to vaccine strains. The high mutation rates of these viruses, coupled with selective pressure from vaccination and poultry management practices, contribute to the ongoing genetic and antigenic evolution. Therefore, the sustained monitoring of genetic mutations in H9N2 viruses is crucial. Continuous surveillance and genetic analyses will be essential to track viral evolution and mitigate potential risks to poultry health, as well as to anticipate any zoonotic threats posed by this adaptable virus.

Acknowledgments

This study was supported by the Razi Vaccine and Serum Research Institute, Karaj, Iran, under grant No. 2-18-18-057-990434.

Conflict of interest

The authors declare that they have no known competing financial interests, personal, or other relationships that could have appeared to influence the work reported in this paper.

References

1. Black EJ, Powell CS, Dempsey DM, et al. Virus taxonomy: the database of the International Committee on Taxonomy of Viruses. Nucleic Acids Res 2026; 54(D1): D776-D789.
2. Swayne ED, Suarez DL, Sims LD. Influenza. In: Swayne DE, Boulianne M, Logue CM, et al. (Eds). Diseases of poultry. 14th ed. New York, USA: John Wiley & Sons 2020; 210-256.
3. Peacock THP, James J, Sealy JE, et al. A global perspective on H9N2 avian influenza virus. Viruses 2019; 11(7): 620. doi: 10.3390/v11070620.
4. Zhang J, Huang L, Liao M, et al. H9N2 avian influenza viruses: challenges and the way forward. Lancet Microbe 2023; 4(2): e70-e71.
5. Peiris M, Yuen KY, Leung CW, et al. Human infection with influenza H9N2. Lancet 1999; 354(9182): 916-917.
6. Xu C, Fan W, Wei R, et al. Isolation and identification of swine influenza recombinant A/Swine/Shandong/1/2003 (H9N2) virus. Microbes Infect 2004; 6(10): 919-925.
7. Fusaro A, Monne I, Salviato A, et al. Phylogeography and evolutionary history of reassortant H9N2 viruses with potential human health implications. J Virol 2011; 85(16): 8413-8421.
8. Bashashati M, Chung DH, Fallah Mehrabadi MH, et al. Evolution of H9N2 avian influenza viruses in Iran, 2017-2019. Transbound Emerg Dis 2021; 68(6): 3405-3414.
9. Bashashati M, Vasfi Marandi M, Sabouri F. Genetic diversity of early (1998) and recent (2010) avian influenza H9N2 virus strains isolated from poultry in Iran. Arch Virol 2013; 158(10): 2089-2100.
10. Hoffmann E, Stech J, Guan Y, et al. Universal primer set for the full-length amplification of all influenza A viruses. Arch Virol 2001; 146(12): 2275-2289.
11. Hall TA. BioEdit: a user-friendly biological sequence alignment editor and analysis program for Windows 95/98/NT. Nucleic Acids Symp Ser 1999; 41: 95-98.
12. Kumar S, Stecher G, Suleski M, et al. MEGA12: molecular evolutionary genetic analysis version 12 for adaptive and green computing. Mol Biol Evol 2024; 41(12): msae263. doi: 10.1093/molbev/msae263.
13. Martin DP, Murrell B, Golden M, et al. RDP4: Detection and analysis of recombination patterns in virus genomes. Virus Evol 2015; 1(1): vev003. doi: 10.1093/ve/vev003.
14. Suchard MA, Lemey P, Baele G, et al. Bayesian phylogenetic and phylodynamic data integration using BEAST 1.10. Virus Evol 2018; 4(1): vey016. doi: 10.1093/ve/vey016.
15. Rambaut A, Drummond AJ, Xie D, et al. Posterior summarization in Bayesian phylogenetics using Tracer 1.7. Syst Biol 2018; 67(5): 901-904.
16. Wan H, Perez DR. Amino acid 226 in the hemagglutinin of H9N2 influenza viruses determines cell tropism and replication in human airway epithelial cells. J Virol 2007; 81(10): 5181-5191.
17. Wan H, Sorrell EM, Song H, et al. Replication and transmission of H9N2 influenza viruses in ferrets: evaluation of pandemic potential. PloS One 2008; 3(8): e2923. doi: 10.1371/journal.pone.0002923.
18. Kaverin NV, Rudneva IA, Ilyushina NA, et al. Structural differences among hemagglutinins of influenza A virus subtypes are reflected in their antigenic architecture: analysis of H9 escape mutants. J Virol 2004; 78(1): 240-249.
19. Okamatsu M, Sakoda Y, Kishida N, et al. Antigenic structure of the hemagglutinin of H9N2 influenza viruses. Arch Virol 2008; 153(12): 2189-2195.
20. Peacock T, Reddy K, James J, et al. Antigenic mapping of an H9N2 avian influenza virus reveals two discrete antigenic sites and a novel mechanism of immune escape. Sci Rep 2016; 6: 18745. doi: 10.1038/srep18745.
21. Peacock TP, Harvey WT, Sadeyen JR, et al. The molecular basis of antigenic variation among A (H9N2) avian influenza viruses. Emerg Microbes Infect 2018; 7(1): 176. doi: 10.1038/s41426-018-0178-y.
22. Wan Z, Ye J, Xu L, et al. Antigenic mapping of the hemagglutinin of an H9N2 avian influenza virus reveals novel critical amino acid positions in antigenic sites J Virol 2014; 88(7): 3898-3901.
23. Bright RA, Shay DK, Shu B, et al. Adamantane resistance among influenza A viruses isolated early during the 2005-2006 influenza season in the United States. JAMA 2006; 295(8): 891-894.
24. Zhang M, Zhao C, Chen H, et al. Internal gene cassette from a human-origin H7N9 influenza virus promotes the pathogenicity of H9N2 avian influenza virus in mice. Front Microbiol 2020; 11: 1441. doi: 10.3389/fmicb.2020.01441.
25. Naffakh N, Tomoiu A, Rameix-Welti MA, et al. Host restriction of avian influenza viruses at the level of the ribonucleoproteins. Annu Rev Microbiol 2008; 62: 403-424.

26. Yao Q, Liu J, Liu H, et al. One-Health challenge in H9N2 avian influenza: novel human-avian reassortment virus in Guangdong province, China. Transbound Emerg Dis 2024; 2024: 9913934. doi: 10.1155/2024/9913934.
27. Li X, Shi J, Guo J, et al. Genetics, receptor binding property, and transmissibility in mammals of naturally isolated H9N2 avian influenza viruses. PLoS Pathog 2014; 10(11): e1004508. doi: 10.1371/journal.ppat.1004508.
28. Bashashati M, Mojahedi Z, Roudsari AA, et al. Ongoing genetic evolution of H9N2 avian influenza viruses in Iranian industrial poultry farms. Acta Vet Hung 2020; 68(3): 328-335.
29. Moosakhani F, Shoshtari AH, Pourbakhsh SA, et al. Phylogenetic analysis of the hemagglutinin genes of 12 H9N2 influenza viruses isolated from chickens in Iran from 2003 to 2005. Avian Dis 2010; 54(2): 870-874.
30. Kim P, Jang YH, Kwon SB, et al. Glycosylation of hemagglutinin and neuraminidase of influenza A virus as signature for ecological spillover and adaptation among influenza reservoirs. Viruses 2018; 10(4): 183.
31. Shi WF, Dun AS, Zhang Z, et al. Selection pressure on haemagglutinin genes of H9N2 influenza viruses from different hosts. Virol Sin 2009; 24(1): 65-70.
32. Li W, Shi W, Qiao H, et al. Positive selection on hemagglutinin and neuraminidase genes of H1N1 influenza viruses. Virol J 2011; 8: 183. doi: 10.1186/1743-422X-8-183.